

Synthesis of Zn and Cd chalcogenides via mechanically induced self-propagating reaction and sonochemical synthesis of PbS

Tsukio Ohtani and Kenta Ishimaru*

Laboratory for Solid State Chemistry, Department of Chemistry, Faculty of Science,

**Graduate School of Science,*

Okayama University of Science,

Ridai-cho 1-1, Kita-ku, Okayama 700-0005, Japan

(Received October 1, 2018; accepted December 6, 2018)

ZnX and CdX (X: S, Se, Te) were prepared by milling the equimolar ratio of elemental mixtures in a planetary ball mill (Fritch P-7) in air atmosphere at room temperature. Wurtzite (ZnS: stable above 1293 K) was synthesized by 20 min of milling via mechanically induced self-propagating reaction (MSR). The wurtzite gradually changed to zinc blende (ZnS: stable below 1293 K) on further milling. ZnSe with wurtzite structure (metastable phase) was obtained by 7 min of milling via MSR. This phase gradually transformed to the stable zinc blende-phase on further milling. Zinc blende-phase of ZnTe was obtained by 20-30 min of milling via MSR. CdS with wurtzite structure (stable phase) was synthesized by 5-10 min of milling via MSR. This phase gradually transformed to metastable zinc blende-phase on subsequent milling. Wurtzite phase of CdSe (stable phase) was obtained by 2-5 min of milling via MSR. This phase gradually changed to zinc blende-phase (metastable) on further milling. CdTe with zinc blende structure was obtained by 10 min of milling probably via MSR. PbS with NaCl structure was obtained by irradiating the elemental mixture in methanol with ultrasound at 45 kHz using a commercial ultrasonic cleaner.

Keywords: mechanical alloying; planetary ball mill; II-VI semiconductor compounds; Zn chalcogenides; Cd chalcogenides; ZnS; ZnSe; ZnTe; CdS; CdSe; CdTe; PbS; zinc blende structure; wurtzite structure; metastable phase; X-ray diffraction method; mechanically induced self-propagating reaction; MSR; sonochemical reaction; ultrasound irradiation; SEM

1. Introduction

Mechanical alloying (MA) method is a high-energy ball milling process involving repeated welding and fracturing of powder particles¹. In high energy milling processes particles are strongly stressed by colliding with each other and contacting with vials and balls. The mechanical energy supplied by the milling is transferred to the particles, introducing strain into the powders. Such a highly activated state reduces the height of energy barrier required to start the reaction, leading to the easy preparation of materials at room temperatures. MA method is one of the useful techniques for preparation of unique materials such as metastable materials², nonequilibrium solid solution³, amorphized intermetallics^{4,5}, etc. This method was originally developed

for preparation of nickel-based superalloys⁶.

Many metal chalcogenides have been prepared by the MA technique from elemental mixtures⁷⁻¹³. ZnS, NiS, and FeS were easily formed on high energy grinding⁷. The high-temperature phase of NiS (stable above 577 K) was formed by the MA, indicating that the relatively high temperatures are generated during grinding metal-sulfur mixtures⁸. Many metastable phases and a high-pressure phase of copper chalcogenides were prepared by MA method⁹.

II-VI semiconductor compounds such as ZnX and CdX (X: S, Se, Te) exhibit large band gaps, making them useful devices for short wavelength applications in optoelectronics. CdTe is used as a γ -ray detector as well as photovoltaics¹⁴.

These compounds have essentially two kinds of

structure of zinc blende-type and wurtzite-type. In Fig. 1 the crystal structures of zinc blende (αZnS) and wurtzite (βZnS) are shown. S atoms are in cubic-close packed (ccp) arrangement in the zinc blende, and in hexagonal-close packed (hcp) arrangement in the wurtzite. In both compounds Zn atoms are tetrahedrally surrounded by S atoms, the tetrahedral sites being alternately occupied by Zn atoms.

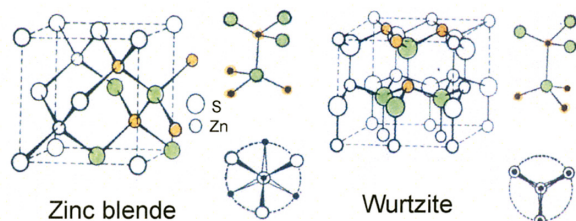


Figure 1. Crystal structures of zinc blende and wurtzite. S atoms are in ccp arrangement in the zinc blende, and are in hcp arrangement in the wurtzite. Zn atoms are tetrahedrally surrounded by S atoms in both structures.

ZnX and CdX (X : S, Se, Te) have been reported to be synthesized by milling the elemental mixtures by many authors. It is particularly noticed that ZnSe and CdSe were synthesized from elemental mixtures via a mechanically induced self-propagating reaction (MSR), where the reaction starts suddenly at a critical time, accompanied by high temperature generation¹⁵. Recently we have observed that when Cd (or Zn) and Se powder was separately pre-milled for 15 min, the elemental mixture reacted to CdSe (or ZnSe) after 5 s of milling, which is much shorter than that for MSR without the pre-milling process¹². These results suggest that in the induction period before the reaction, the mechanical energy supplied by the ball-milling process was employed primarily for activation of the elemental particles.

Sonochemical reaction is induced by irradiating ultrasound to the reactants. Shock waves induced by the acoustic cavitation in liquid-solid slurries produce high-velocity interparticle collisions, leading to chemical reactions¹⁶. We have previously applied this technique to the preparation of copper and silver chalcogenides¹⁷ and $\text{Pd}_{17}\text{Se}_{15}$ ¹¹.

In the present work we prepared ZnX and CdX by milling the elemental mixtures using a planetary ball mill. It was found that stable phases as well as metastable phases were easily obtained by this

method. PbS was prepared by irradiating the methanol-elemental mixture slurry with ultrasound.

2. Experiments

ZnX and CdX were synthesized by milling elemental mixtures with equimolar ratio using a planetary ball mill (Fritsch P-7) in air at room temperature under the following conditions: vial and ball material, tungsten carbide; inner volume of the vial, 25 mL; ball charge, 4 balls of tungsten carbide with 10 mm diameter; weight of starting mixtures, ~ 0.6 g; rotational speed of the planet carrier, 580 rpm; milling time, up to 60 min.

Figure 2 shows a central part of Fritsch P-7, consisting of two grinding vials arranged eccentrically on the supporting disc. The direction of movement of the supporting disc is opposite to that of the grinding vials. As shown in Fig. 3, the large centrifugal force induced by the rotation has higher impact energy.

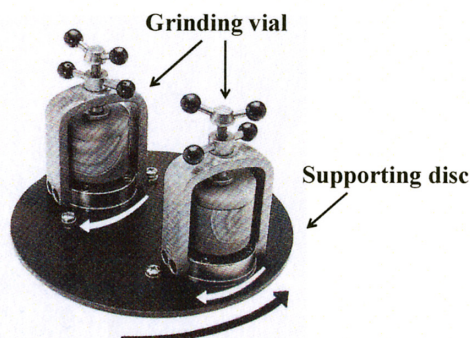


Figure 2. Planetary ball mill (Fritsch P-7). Grinding vials and supporting disc turn in opposite directions.

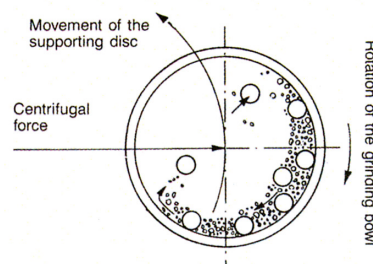


Figure 3. The illustration of inside of grinding vial in planetary ball mill (Fritsch P-7).

The schematic illustration of a setup for sonochemical synthesis is shown in Fig. 4. The elemental mixture with equimolar ratio (0.3 g in weight) was

immersed in 1.0 mL of methanol contained in a glass tube with inner diameter of 8.0 mm. The tube was partly submerged in 1.5 dm³ of water in a commercial ultrasonic cleaner (Shimazu, SUS-103; 100 W). The methanol-elemental mixture slurry was irradiated with ultrasound at 45 kHz at room temperature.

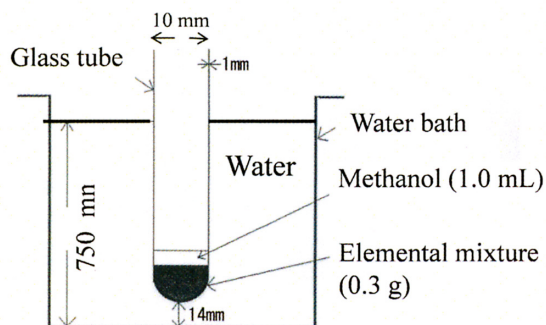


Figure 4. Schematic illustration of a setup for sonochemical synthesis using an ultrasonic cleaner.

The starting elements used were Zn (Wako Pure Chemicals Ltd, 99.9%, powder), Cd (Wako Pure Chemicals Ltd, 99.999%, powder), Pb (Nakalai Tesque, 99%, powder), S (Nakalai Tesque, 99.999%, ingot), Se (Rare Metallic Co., Ltd, 99.9999%, ingot) and Te (Wako Pure Chemicals Ltd, 99.999%, ingot). S, Se, and Te ingots were ground into a powder with a ca. 50 mesh size using an agate mortar prior to the ball milling. The samples obtained were analyzed by powder X-ray diffraction (XRD) using a diffractometer RAD-B (RIGAKU) with CuK α radiation. Scanning electron microscopy (SEM) observations were carried out by using a JEOL JXA-8900 instrument.

3. Results and discussion

3-1 Mechanical alloying synthesis of ZnS

ZnS has two stable phases of α ZnS (zinc blende; stable at < 1293 K) and β ZnS (wurtzite; stable at > 1293 K)¹⁸. Figure 5 gives XRD patterns of Zn-S after various periods of ball milling of elemental mixture. No reaction was observed by milling for 20 min. After 25 min of milling, the wurtzite suddenly appeared. On further milling, the pattern of wurtzite gradually changed to that of zinc blende. Almost single phase of zinc blende was obtained by 60 min of milling. The transition from wurtzite to zinc blende has been already observed in MA of Zn-S^{19, 20}.

It is notable that the starting mixture suddenly re-

acted to the wurtzite phase between 20 and 25 min of milling, suggesting that the compound was produced via MSR (mechanically induced self-propagating reaction). XRD patterns of Zn-S obtained by milling the elemental mixture from 15 to 20 min are shown in Fig. 6. The reaction occurred between 19 and 20 min of milling, exhibiting that the product was produced by the MSR. The discrepancy on the starting reaction-time between Fig. 5 and Fig. 6 may be due to the small difference of experimental conditions.

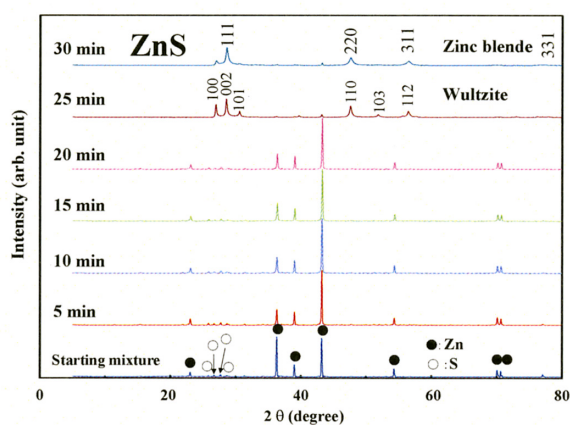


Figure 5. XRD patterns of Zn-S obtained by ball milling of elemental mixture for various periods.

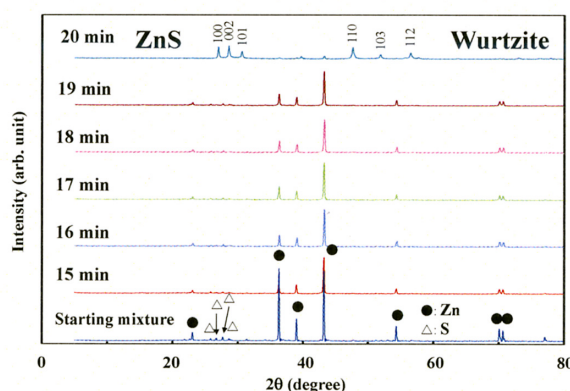


Figure 6. XRD patterns of Zn-S obtained by milling the elemental mixture every 1 min. The wurtzite phase appeared suddenly between 19 and 20 min.

The MSR resembles to the self-propagating high-temperature reaction (SHS). For the SHS, the adiabatic temperature, defined as the final temperature, is used as a measure of self-heating. For MSR, the quantity $-\Delta H_{298}/C_{298}$ (ΔH_{298} : reaction enthalpy, C_{298} : heat capacity) is often used as a simpler substi-

tute for the adiabatic temperature¹⁵). MSR occurs in the condition of $-\Delta H_{298}/C_{298} > 2000$ K for all materials¹⁵). Using available data, the value of $-\Delta H_{298}/C_{298}$ for ZnS (zinc blende) was estimated to be 3570 K, confirming the MSR. The value for wurtzite would not be so different from that of zinc blende.

Figure 7 (a) and (b) show SEM images of ZnS obtained by milling the elemental mixture for 19 min and for 20 min, respectively. The particles in Fig. 7 (b) seem to be aggregates of much smaller particles than those of Fig. 7(a), indicating the mixture was suddenly reacted by milling for 19-20 min.

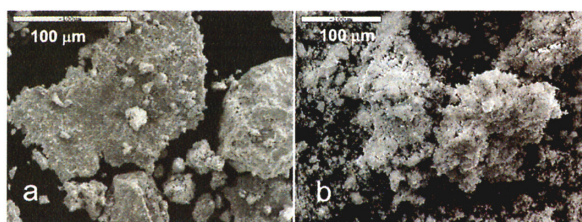


Figure 7. SEM images of ZnS obtained by milling for 19 min (a), and for 20 min (b). The abrupt morphology change shows that the reaction is of the MRS type. Scale bars indicate 100 μm .

3-2 Mechanical alloying synthesis of ZnSe

ZnSe occurs mainly in two phases: one with zinc blende structure (αZnSe : stable)²¹) and the other with wurtzite structure (metastable)²²). The latter is able to be obtained by vapor deposition²²). ZnSe has been prepared by MA method²³⁻²⁸).

Figure 8 shows XRD patterns of Zn-Se obtained by milling the elemental mixture of Zn and amorphous Se for different times. The wurtzite phase suddenly appeared after 7 min of milling, indicative of the MSR. Preparations via MSR of ZnSe have been already reported in many literatures^{12,29,30}). The wurtzite phase gradually changed to the zinc blende phase on further milling. As shown in Fig 9, the almost single phase of zinc blende-type was obtained by 20 min of milling. The value of $-\Delta H_{298}/C_{298}$ for ZnSe was estimated to be 3084 K¹²).

Figure 10 gives SEM images of Zn-Se particles obtained by 6 min of milling (a) and 7 min of milling (b) of elemental mixture. The particles obtained by 6 min of milling seem to be unreacted, but those obtained by 7 min of milling seem to be uniformly reacted powders, apparently indicating the reaction is

of MSR. Morphological change induced by MSR on this compound was observed more clearly by HAADF-STEM images¹²).

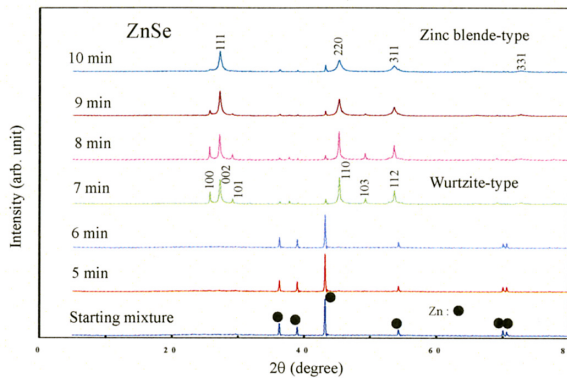


Figure 8. XRD patterns of Zn-Se obtained by milling the elemental mixture (Zn + Se) for various periods.

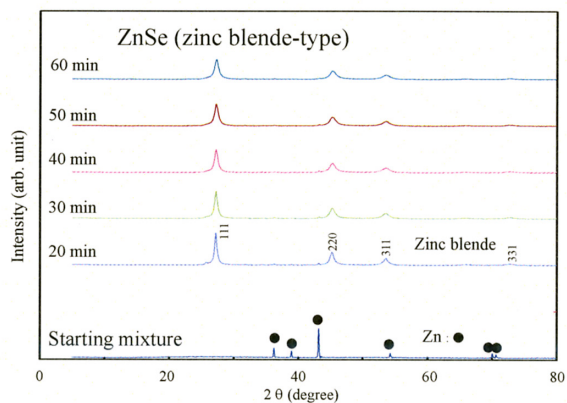


Figure 9. XRD patterns of Zn-Se obtained by milling the elemental mixture for various periods.

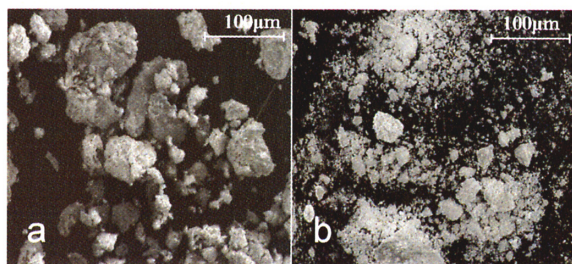


Figure 10. SEM images of Zn-Se particles obtained by milling the elemental mixture for 6 min (a), and for 7 min (b). The sudden morphology change suggests the reaction was promoted by MRS. Scale bars indicate 100 μm .

3-3 Mechanical alloying synthesis of $\text{Zn}(\text{S}_{1-x}\text{Se}_x)$

Figure 11 gives XRD patterns of $\text{Zn}(\text{S}_{1-x}\text{Se}_x)$ ob-

tained by milling the elemental mixture for 30 min. All patterns show the zinc blende structure. Calculated lattice parameter of ZnS and ZnSe were $a = 0.5390$ nm and 0.5660 nm, respectively, which are consistent with reference values^{31,32}.

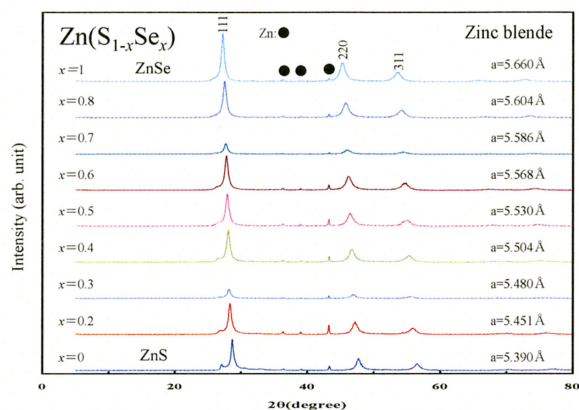


Figure 11. XRD patterns of $Zn(S_{1-x}Se_x)$ system obtained by milling the elemental mixture of Zn, S, and Se for 30 min.

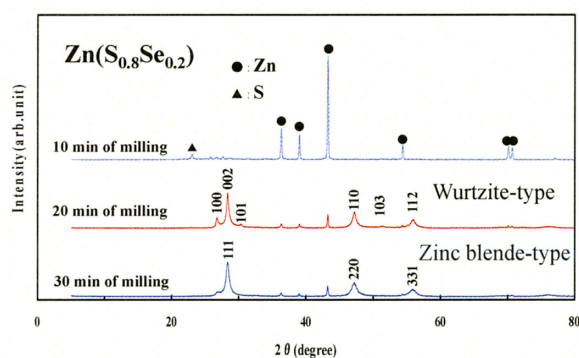


Figure 12. XRD patterns of $Zn(S_{0.8}Se_{0.2})$ obtained by milling the elemental mixture for various periods.

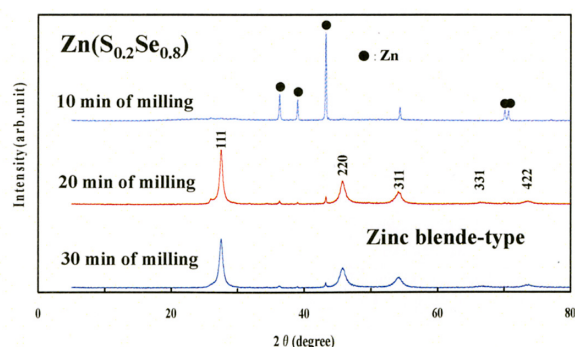


Figure 13. XRD patterns of $Zn(S_{0.2}Se_{0.8})$ obtained by milling the elemental mixture (Zn, S, Se) for various periods.

Figure 12 gives XRD patterns of $Zn(S_{0.8}Se_{0.2})$ ob-

tained by milling the elemental mixture for different times. The wurtzite phase formed by milling between 10 and 20 min, and then transformed to the zinc blende-phase after 30 min of milling. It is noticed that the reaction did not start before 10 min of milling, in spite of that the wurtzite phase was formed by 7 min of milling for ZnSe. Figure 13 shows XRD patterns of $Zn(S_{0.2}Se_{0.8})$ obtained by MA. Zinc blende-phase appeared between 10 and 20 min of milling. For the other compositional samples of $0.3 \leq x \leq 0.7$, the reaction was also observed to start between 10 and 20 min of milling, suggesting that ZnS and ZnSe do not start to react independently, but three elements start to react at the same time via MSR.

Figure 14 shows x dependence of parameter a of zinc blende-type of $Zn(S_{1-x}Se_x)$ system. The parameter almost linearly changes with x , obeying the Vegard's rule, indicating that this system has a complete solid solution.

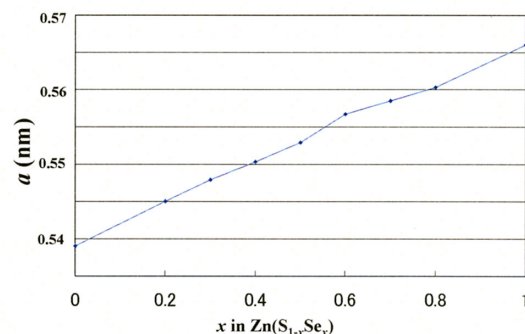


Figure 14. Lattice parameter a vs. x in $Zn(S_{1-x}Se_x)$ with zinc blende structure obtained by milling the elemental mixtures for 30 min

3-4 Mechanical alloying synthesis of ZnTe

ZnTe has mainly a zinc blende-phase (α ZnTe)^{33,34}. ZnTe has been synthesized recently by MA method^{35,36}. Figure 15 shows XRD patterns of Zn-Te obtained by milling the elemental mixture for different times. After 10 min of milling, a small amount of zinc blende-phase appeared. The amount of this phase suddenly increases between 10 and 20 min of milling. Small amounts of Zn and Te together with ZnO were detected even after 30 min of milling. This reaction seems to be of the MSR type, because the reaction did not proceed by subsequent milling after 20 min. By using available thermodynamic data of ZnTe, the adiabatic temperature of $-\Delta H_{298}/C_{298}$ was

estimated to be 2315 K, suggesting the MSR.

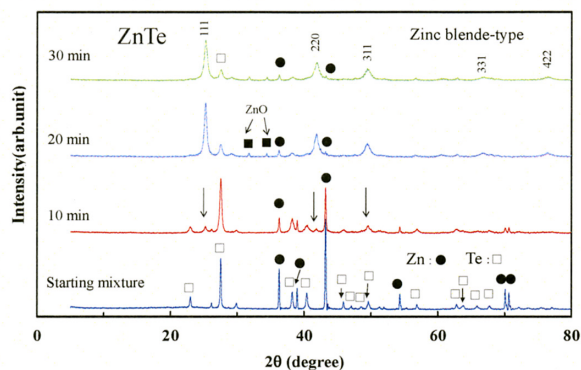


Figure 15. XRD patterns of Zn-Te obtained by milling the elemental mixture for different periods.

3-5 Mechanical alloying synthesis of CdS

Stable phase of α CdS has wurtzite-type structure³⁷⁾. When prepared by vapor deposition or from aqueous solution, CdS forms as a metastable zinc blende-phase³⁷⁾. Wurtzite phase of CdS was obtained by milling the elemental mixture³⁸⁾. Figure 16 gives XRD patterns of Cd-S obtained by milling the elemental mixture for different times. The wurtzite phase appeared after 10 min of milling. This phase was not observed by 5 min of milling, indicating that the reaction suddenly occurred by milling between 5 and 10 min, suggesting that the reaction is of the MSR type. The value of $-\Delta H_{298}/C_{298}$ for CdS was estimated to be 2380 K, confirming the MSR. On further milling the wurtzite phase gradually transformed to the metastable zinc blende phase.

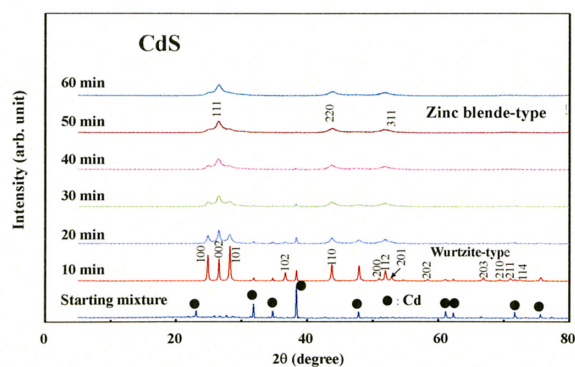


Figure 16. XRD patterns of Cd-S obtained by milling the elemental mixture for various periods.

3-6 Mechanical alloying synthesis of CdSe

CdSe has mainly two phases with the wurtzite structure (stable)³⁹⁾ and the zinc blende structure (metastable)⁴⁰⁾. MA synthesis of CdSe has been already reported by some authors^{23,24)}. We have recently reported the wurtzite phase appeared via MSR by 2 min of milling using Fritch P-7¹²⁾. Figure 17 shows XRD patterns for Cd-Se obtained by milling the elemental mixture for various periods. The wurtzite phase appeared after 5 min of milling. On subsequent milling, the wurtzite phase gradually transformed to the zinc blende phase.

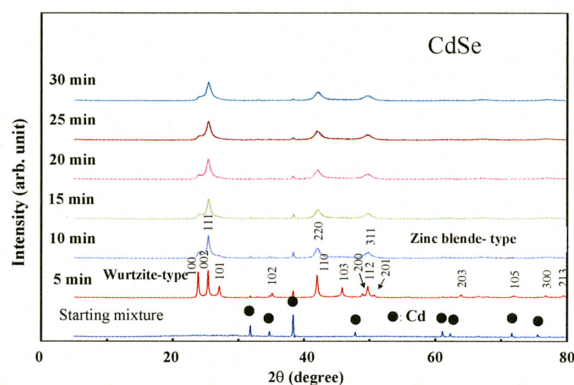


Figure 17. XRD patterns for Cd-Se obtained by milling the elemental mixture for different periods.

3-7 Mechanical alloying synthesis of CdTe

CdTe has mainly two phases: a stable phase with zinc blende structure^{41,42)} and a metastable phase with wurtzite structure⁴³⁾. MA synthesis of CdTe has been reported in earlier literatures⁴⁴⁾. Figure 18 shows XRD patterns for Cd-Te obtained by milling the elemental mixture for different times. Zinc blende-phase appeared in 10 min of milling. Almost single phase of zinc blende-type was obtained by 30 min of milling.

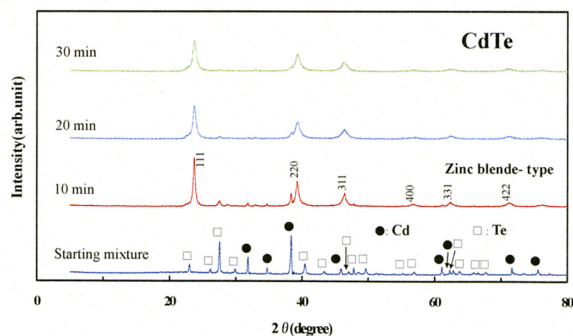


Figure 18. XRD patterns for Cd-Te obtained by milling the elemental mixtures for various periods.

The value of $-\Delta H_{298}/C_{298}$ for CdTe was estimated to be 1835 K, which is somewhat smaller than the criterion value of 2000 K for the occurrence of MSR. However, the sudden appearance of CdTe as well as no further reaction after 10 min of milling suggests that the reaction is promoted by MSR. The wurtzite phase was not obtained in the present study.

3-8 MA and Sonochemical syntheses of PbS

PbS forms a stable phase with NaCl structure⁴⁵. MA synthesis of PbS has been already reported⁴⁶. Figure 19 shows XRD patterns of Pb-S obtained by milling the equimolar ratio of elemental mixture. PbS appeared by 5 min of milling, and the single phase was obtained by 30 min of milling. The value of $-\Delta H_{298}/C_{298}$ for PbS was estimated to be 2140 K, suggesting the MSR, although the amount of Pb gradually decreases with milling time after 5 min.

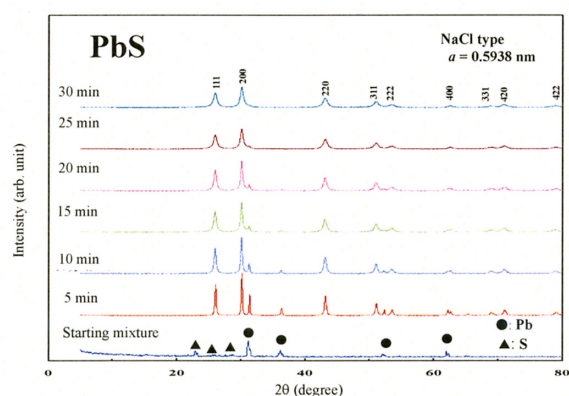


Figure 19. XRD patterns of Pb-S obtained by milling the elemental mixture.

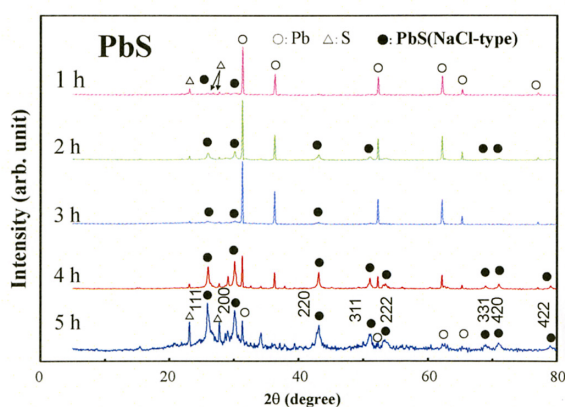


Figure 20. XRD patterns of Pb-S obtained by irradiating the elemental mixture in methanol with ultrasound at 45 kHz for different times at room temperature.

Figure 20 shows XRD patterns of Pb-S obtained by irradiating the elemental mixture of equimolar ratio in methanol with ultrasound at 45 kHz for different times. PbS gradually appeared with increasing the time of ultrasonic irradiation. The starting elements of Pb and S, however, remain even after 5h of milling. PbS was not able to be obtained by irradiation of ultrasound at both 28 kHz and 100 kHz.

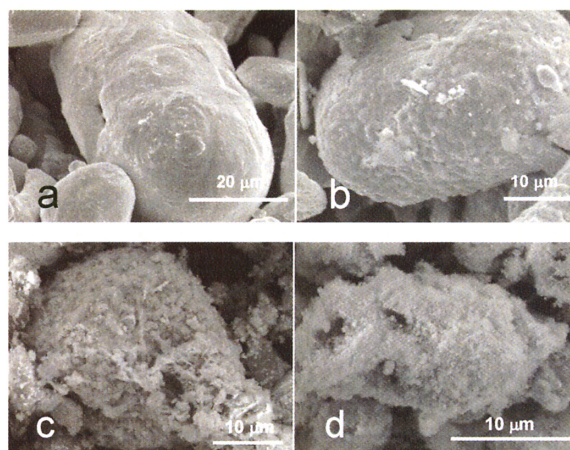


Figure 21. SEM images of Pb particles obtained by irradiating the elemental mixture (Pb + S) in methanol with ultrasound at 45 kHz: (a) before irradiation, (b) after 3 h of irradiation, (c) after 4 h of irradiation, (d) after 5 h of irradiation. Scale bars indicate 20 μm (a), and 10 μm (b, c, d).

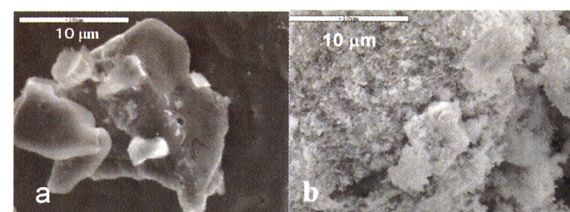


Figure 22. SEM images of S particles: (a) starting S particles. (b) S particles after irradiating the elemental mixture (Pb + S) in methanol with ultrasound at 45 kHz for 5 h. Scale bars indicate 10 μm for both figures.

Figure 21 shows SEM images of Pb particles obtained by irradiating the elemental mixture of Pb and S with ultrasound at 45 kHz at room temperature. With increasing irradiation time, the smooth surfaces of starting Pb particles changed to rough ones, and the round shape of the starting particles changes to deformed shape covered with aggregates of small irregular particles. These results clearly show that the reaction proceeded with increasing the irradiation

time. These images resemble to our previous results of sonochemical synthesis of Cu and Ag chalcogenides¹⁷⁾, where the reaction proceeded from the surface to the inside of each particle with increasing the irradiation time, exhibiting a clear boundary between the pure elements and the products⁴⁷⁾. It may be also the case in the present study, although we have not observed the inside of the particles.

Figure 22 shows SEM images of starting S particles (a) and SEM images after irradiating the elemental mixture (Pb and S) with ultrasound for 5 h (b). Like Pb particles, the S particles after 5 h of irradiation are covered with smaller grains.

We have failed to prepare the following compounds by the sonochemical method presently used: BiS (45 kHz), BiSe (45 kHz), CdS (28 kHz, 45 kHz, 100 kHz), CdSe (28 kHz, 45 kHz, 100 kHz), GeS (45 kHz), GeSe (45 kHz), PbSe (45 kHz), SnS (45 kHz), SnSe (45 kHz), ZnS (28 kHz, 45 kHz, 100 kHz), ZnSe (28 kHz, 45 kHz, 100 kHz).

4. Summary

ZnX and CdX (X: S, Se, Te) were prepared by milling the equimolar ratio of elemental mixtures using a planetary ball mill (Fritsch P-7) in air atmosphere at room temperature. Obtained results are briefly summarized as follows.

ZnS:

- Wurtzite phase (high-temperature phase) was obtained by 20 min of milling via MSR.
- Zinc blende-phase (low-temperature phase) was obtained by 30 min of milling.

ZnSe:

- Wurtzite phase (metastable) was obtained by 7 min of milling via MSR.
- Zinc blende-phase (stable) was obtained by 10 min of milling.

ZnTe:

- Zinc blende-phase (stable) was obtained by 30 min of milling via MSR.
- Wurtzite phase does not exist.

CdS:

- Wurtzite phase (stable) was obtained by 5 min of milling via MSR.
- Zinc blende-phase (metastable) was obtained by 30-60 min of milling.

CdSe:

- Wurtzite phase (stable) was obtained by 2 min of

milling via MSR.

- Zinc blende-phase (metastable) was obtained by ~30min of milling.

CdTe:

- Wurtzite phase (metastable) was not obtained.
- Zinc blende-phase (stable) was obtained by 10 min of milling possibly via MSR.

These results for ZnX and CdX are summarized in Table I. Existing phases including metastable phases were prepared by MA, except for the tellurides. It was observed commonly in these compounds except for the tellurides that the wurtzite phase was first prepared via MSR, regardless that each wurtzite phase are in the stable or in the metastable state. The MSR may give some preferable influences for the production of the wurtzite phase rather than the zinc blende phase.

Table I. Preparation results of ZnX and CdX (X: S, Se, Te) obtained by milling the elemental mixtures in planetary ball mill (Fritsch P-7) at room temperature; the mark “○+MSR” indicates the successful preparation via MSR, the mark “○” the occurrence of zinc blend-phase on further milling after the appearance of wurtzite phase, and the mark “×” unsuccessful preparation.

		ZnS	ZnSe	ZnTe	CdS	CdSe	CdTe
Zinc blende type	Published data	Stable < 1293K	Stable	Stable	Meta-stable	Meta-stable	Stable
	Present results	○	○	○ MSR	○	○	○ MSR
Wurtzite type	Published data	Stable > 1293K	Meta-stable	—	Stable	Stable	Meta-stable
	Present results	○ MSR	○ MSR	—	○ MSR	○ MSR	×

PbS with NaCl structure was obtained by milling the elemental mixture for 30 min using Fritsch P-7. This phase was also obtained by irradiating the elemental mixture in methanol with ultrasound at 45 kHz using a commercial ultrasonic cleaner.

This paper was prepared based on the master's thesis for graduate school of science submitted by Kenta Ishimaru (2012).

References

- 1) C. Suryanarayana, *Rev. Adv. Mater. Sci.*, **18**, 203 (2008).
- 2) H. J. Fecht, G. Han, Z. Fu, and W. L. Johnson, *J. Appl. Phys.*,

- 67, 1744 (1990).
- 3) A. O. Aning, Z. Wan, and T. H. Courtney, *Acta Metall. Mater.*, **41**, 165 (1993).
 - 4) L. Shultz, *Mater. Sci. Eng.*, **97**, 15 (1988).
 - 5) R. B. Schwarz, *Mater. Sci. Eng.*, **97**, 71 (1988).
 - 6) J. S. Benjamin, *Metall. Trans.*, **1**, 2943 (1970).
 - 7) T. Kosmac, and T. H. Courtney, *J. Mater. Res.*, **7**, 1519 (1992).
 - 8) T. Kosmac, D. Maurice, and T. H. Courtney, *J. Am. Ceram. Soc.*, **76**, 2345 (1993).
 - 9) T. Ohtani, M. Motoki, K. Koh, and K. Ohshima, *Mater. Res. Bull.*, **30**, 1495 (1995).
 - 10) T. Ohtani, K. Maruyama, and K. Ohshima, *Mater. Res. Bull.*, **32**, 343 (1997).
 - 11) T. Ohtani, K. Ikeda, Y. Hayashi, and Y. Fukui, *Mater. Res. Bull.*, **42**, 1930 (2007).
 - 12) T. Ohtani, Y. Kusano, K. Ishimaru, T. Morimoto, A. Togano, and T. Yoshioka, *Chem. Letters*, **44**, 1234 (2015).
 - 13) P. Baláž, “*Mechanochemistry in Nanoscience and Minerals Engineering*”, Springer-Verlag, Berlin, Heidelberg (2010).
 - 14) F. V. Wald, *Revue de Physique Appliquee*, **12**, 277 (1977).
 - 15) L. Takacs, *Prog. Mater. Sci.*, **47**, 355 (2002) and references therein.
 - 16) K. S. Suslick, *Science*, **247**, 1439 (1990).
 - 17) T. Ohtani, T. Nonaka, and M. Araki, *J. Solid State Chem.*, **138**, 131 (1998).
 - 18) T. B. Massalski (editor-in-chief), *Binary Alloy Phase Diagrams (2nd ed.)*, ASM International, Ohio, pp. 3297 (1990).
 - 19) M. Senna, *Crystal Res. Technol.*, **20**, 209 (1985).
 - 20) P. Balaz, M. Balintova, Z. Bastl, J. Briancin, and V. Sepelak, *Solid State Ionics*, **101-103**, 45 (1997).
 - 21) T. B. Massalski (editor-in-chief), *Binary Alloy Phase Diagrams (2nd ed.)*, ASM International, Ohio, pp. 3357 (1990).
 - 22) Y. S. Park and F. L. Chan, *J. Appl. Phys.*, **36**, 800 (1965).
 - 23) G. L. Tan, J. H. Du, and Q. J. Zhang, *J. Alloy Comp.*, **468**, 421 (2009).
 - 24) G. L. Tan and R. H. Liu, *J. Nanoparticle Res.*, **12**, 605 (2010).
 - 25) G. A. da Silva, D. M. Triches, E. A. Sanches, K. D. Machad, C. M. Poffo, J. C. de Lima, and S. M. de Souza, *J. Mol. Str.*, **1074**, 511 (2014).
 - 26) J. C. de Lima, V. H. F. dos Santos, and T. A. Grandi, *Nanostruct. Mater.*, **11**, 51 (1999).
 - 27) J. Baltazar-Rodrigues, J. C. de Lima, C. E. M. Campos, and T. A. Grandi, *Powder Technol.*, **189**, 70 (2009).
 - 28) M. Achimovicova, P. Balaz, T. Ohtani, N. Kostova, G. Tyuliev, A. Feldhoff, and V. Sepelak, *Solid State Ionics*, **192**, 632 (2011).
 - 29) Chr. G. Tschakarov, G. G. Gospodinov, and Z. Bontschev, *J. Solid State Chem.*, **41**, 244 (1982).
 - 30) F. J. Gotor, M. Achimovicova, C. Real, and P. Balaz, *Powder Tech.*, **233**, 1 (2013).
 - 31) JCPDS data (File No. 05-0566).
 - 32) JCPDS data (File No. 05-0522).
 - 33) T. B. Massalski (editor-in-chief), *Binary Alloy Phase Diagrams (2nd ed.)*, ASM International, Ohio, pp. 3474 (1990).
 - 34) JCPDS data (File No. 15-0746).
 - 35) C. E. M. Campos, J. C. de Lima, T. A. Grandi, and H. Höhn, *J. Noncrst. Solids*, **354**, 3503 (2008).
 - 36) S. Patra and S. K. Pradhan, *Acta Materialia*, **60**, 131 (2012).
 - 37) T. B. Massalski (editor-in-chief), *Binary Alloy Phase Diagrams (2nd ed.)*, ASM International, Ohio, pp. 1020 (1990).
 - 38) G. L. Tan, L. Zhang, X. F. Yu, *J. Phys. Chem. C*, **114**, 290 (2010).
 - 39) R. A. Reisman, M. Berkenblit, and M. Witzten, *J. Phys. Chem.*, **66**, 2210 (1962).
 - 40) R. B. Kale and C. D. Lokhande, *J. Phys. Chem. B*, **109**, 20288 (2005).
 - 41) T. B. Massalski (editor-in-chief), *Binary Alloy Phase Diagrams (2nd ed.)*, ASM International, Ohio, pp. 1032 (1990).
 - 42) JCPDS data (File No. 15-0770).
 - 43) C. Kaito, K. Fujita, and M. Shiojiri, *J. Cryst. Growth*, **62**, 375 (1983).
 - 44) G. L. Tan, Q. Yang, U. Hömmerich, J. T. Seo, and D. Temple, *Optical Mater.*, **27**, 579 (2004).
 - 45) T. B. Massalski (editor-in-chief), *Binary Alloy Phase Diagrams (2nd ed.)*, ASM International, Ohio, pp. 3005 (1990).
 - 46) P. Balaz, E. Godocikova, P. Lobotzka, and E. Gock, *Mater. Sci. Eng. A*, **386**, 442 (2004).
 - 47) T. Ohtani, M. Araki, and M. Shohno, *Solid State Ionics*, **172**, 197 (2004).

